Supplementary Information

Arene C-H activation using Rh (I) Catalysts Supported by Bidentate Nitrogen Chelates

Michael. S. Webster-Gardiner,[a] Ross. Fu,[b] G. C. Fortman,[a] R. J. Nielsen,[b] T. Brent. Gunnoe,[a*] and William. A. Goddard III[b*]
Department of Chemistry, University of Virginia, Charlottesville, Virginia 22904, United States[a],
Department of Chemistry, California Institute of Technology, Pasadena, California 91125, United States [b]

Table of Contents

Experimental Details

Computational Details

General Considerations. Unless otherwise noted, all synthetic procedures were performed under anaerobic conditions in a nitrogen-filled glovebox or by using standard Schlenk techniques. Glovebox purity was maintained by periodic nitrogen purges and was monitored by an oxygen analyzer ($O_2 < 15$ ppm for all reactions). Tetrahydrofuran and *n*–pentane were dried by distillation from sodium/benzophenone. Benzene was purified by passage through a column of activated alumina. C_6D_6 and DMSO-d_6 were used as received and stored under a N_2 atmosphere over 4 Å molecular sieves. [D_1] trifluoroacetic acid and DMF-d_7 was used as received. Argon was purchased from GTS Welco and used as purchased. ^{1}H and ^{13}C NMR spectra were recorded on a Varian Mercury Plus 300 MHz spectrometer (75 MHz operating frequency for ^{13}C NMR), Varian Inova 500 MHz spectrometer (75 MHz operating frequency for ^{13}C NMR), Bruker Avance DRX 600 MHz spectrometer (201 MHz operative frequency for ^{13}C NMR), or Bruker Avance III 800 MHz spectrometer (201 MHz operative frequency for ^{13}C NMR). All ^{1}H and ^{13}C NMR spectra are referenced against residual proton signals (^{1}H NMR) or the ^{13}C resonances of the deuterated solvent (^{13}C NMR). ^{19}F NMR (operating frequency 282 MHz) spectra were obtained on a Varian Mercury 300 MHz spectrometer and referenced against an external standard of hexafluorobenzene (δ −164.9). GC/MS analysis was performed using a Shimadzu GCMS–QP2010 Plus system with a 30 mm × 025 mm RTx-Qbond column with 8 μm thickness using electron impact ionization. All other reagents were used as purchased from commercial sources. The preparation of ligand ^{Fl}DAB has been previously reported.[1] $(COE)_2Rh(TFA)$ was made following the literature procedure using AgTFA instead of $AgPF_6$.[2] H/D exchange was monitored by analysis of GC-MS and an excel sheet developed by Periana and co-workers.[3]

(^{Fl}DAB)Rh(COE)(TFA) (1). To a round bottom flask was added a stir bar, $[Rh(TFA)(COE)_2]_2$ (270 mg, 309 μmol) and 10 mL of THF to give a brown/yellow solution. Then ^{Fl}DAB (258 mg, 619 μmol) was added, and the solution immediately turned dark purple. The solution was stirred for 1 hour before the solvent was removed in vacuo. The residue was washed with 10 mL of pentane. The purple solid was dried under vacuum (274 mg, yield of 58%) and stored in the glovebox freezer. Extensive time under vacuum results in removal of cyclooctene. An interesting observation by ^{1}H NMR spectroscopy is that the methyl groups of the ^{Fl}DAB ligand shift dramatically when coordinated to the metal centre. Free ^{Fl}DAB in C_6D_6 has a resonance at 2.14 ppm whereas the methyl of **1** appears at -1.58 ppm. This has also been shown when ^{Fl}DAB is coordinated to nickel.[1] ^{1}H NMR (600 MHz, THF-d_8) δ -0.44 (s, 6H, CH_3). ^{13}C NMR (201 MHz, DMF-d_7) δ 163.8 (imine N=*C*-CH$_3$), 142.0 (d, $^3J_{CF}$ = 7.7 Hz, *o*-C_6F_5), 140.8 (d, $^3J_{CF}$ = 5.0 Hz, *o*-C_6F_5), 139.6 (t, $^3J_{CF}$ = 13.3 Hz, *p*-C_6F_5), 139.0 (t, $^3J_{CF}$ = 14.6 Hz, *m*-C_6F_5), 137.8 (t, $^3J_{CF}$ = 12.7 Hz, *m*-C_6F_5), 129.9 (*ipso*-C_6F_5), 115.78 (q, $^1J_{CF}$ = 292.9 Hz, *C*F$_3$ TFA), 20.8 (s, *C*H$_3$), 13.7 (q, $^3J_{CF}$ = 22.6 Hz, *C*=O TFA). ^{19}F NMR (282 MHz, DMSO-d_6) δ -74.0 (s, TFA), -151.9 (dd, *J* = 24, 6 Hz, *p* C–F), -162.3 (t, *J* = 23 Hz, *m* C–F), -163.4 (td, *J* = 23, 6 Hz, *o* C–F). Analytical Calc. (without COE, which is removed upon extended drying *in vacuo*) C: 34.20 H: 0.96 N: 4.43 Found: C: 33.61 H: 1.05 N: 4.14.

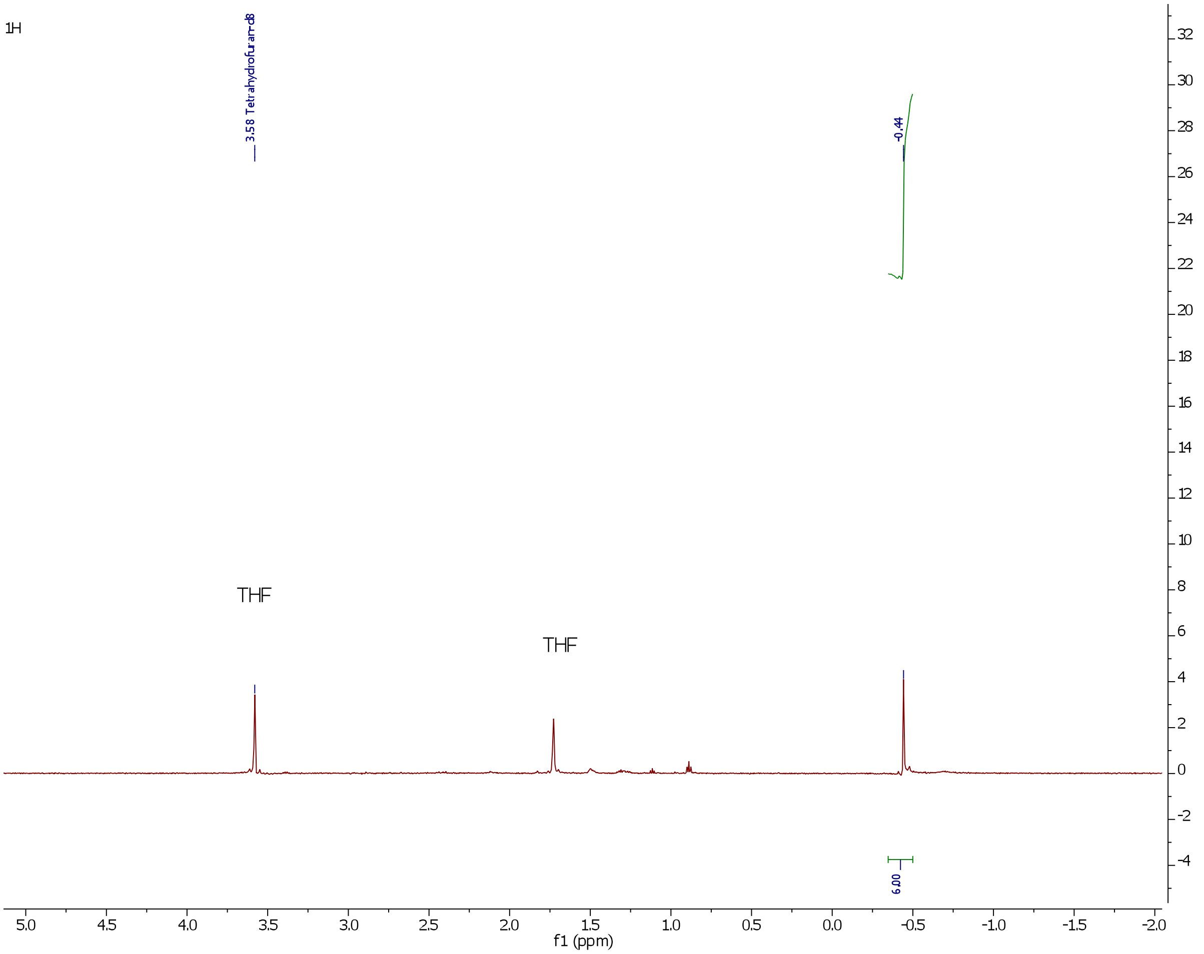

Figure S1. ^{1}H NMR spectrum of (^{Fl}DAB)Rh(COE)(TFA) in THF-d_8.

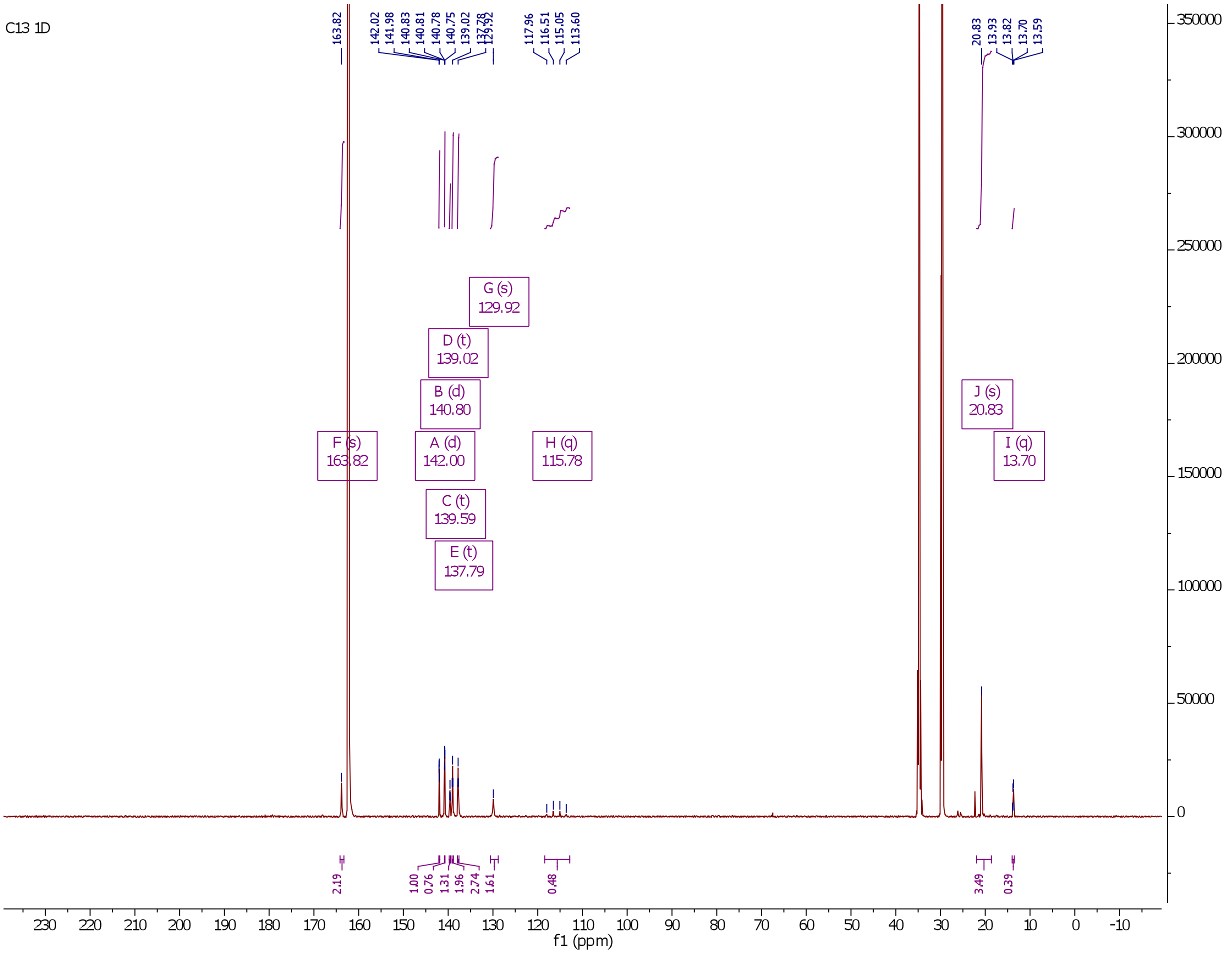

Figure S2. ^{13}C NMR spectrum of (^{Fl}DAB)Rh(COE)(TFA) in DMF-d_7.

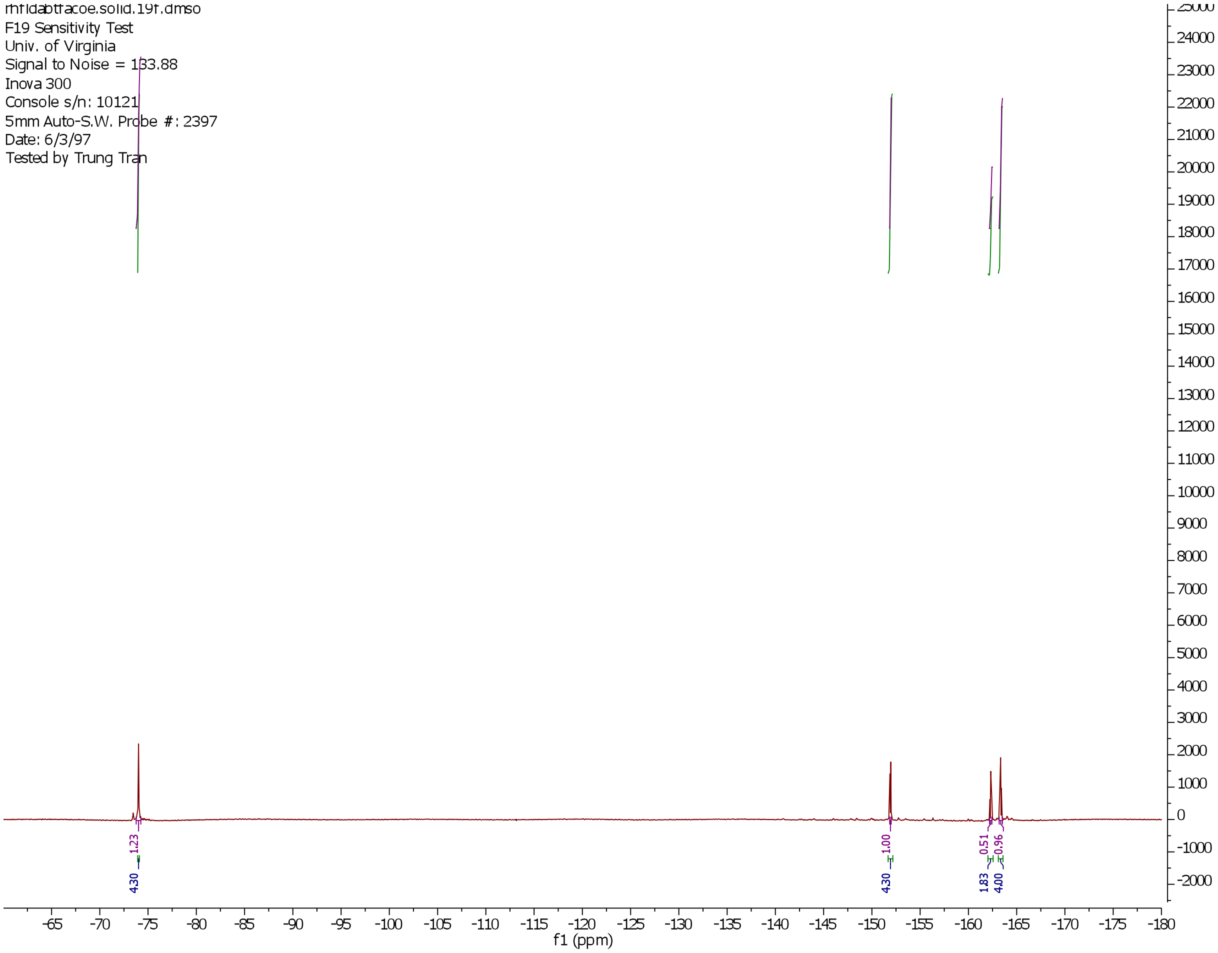

Figure S3. ^{19}F NMR spectrum of Rh(^{Fl}DAB)tfa(COE) in DMSO-d_6.

(BOZO)Rh(COE)(TFA) (2). To a round bottom flask was added a stir bar, $[Rh(TFA)(COE)_2]_2$ (99 mg, 114 µmol), and 10 mL of THF to give a purple solution. BOZO (32 mg, 227 µmol) was added, and the solution immediately turned dark purple. The solution was stirred for 1 hour before the solvent was removed in vacuo. The residue was then washed with 10 mL of pentane. The purple solid was dried under vacuum (59 mg, 73%) and stored in the glovebox freezer. Attempts to obtain clean elemental analysis data were thwarted by the instability of complex **2**. In addition, *in vacuo* complex **2** slowly releases cyclooctene, which complicates efforts to remove solvent. ^{1}H NMR (600 MHz, C_6D_6) δ 3.48 (t, $^3J_{HH}$ = 10 Hz, 2H, O–CH_2), 3.27 (m, 4H, O–CH_2 and N–CH_2, coincidental overlap), 2.27 (bs, 4H, COE), 2.12 (t, , $^3J_{HH}$ = 10 Hz, 2H, N–CH_2), 1.58 (bs, 10H, COE). ^{13}C NMR (201 MHz, DMSO-d_6) δ 160.2 (O-C=N), 158

(*C*=O of TFA), 129.7 (*C*=*C* of COE), 114.9 (q, $^{1}J_{CF}$ = 290 Hz, CF_3), 72.7 (O–CH_2), 53 (N–CH_2), 28.7 (α–*C*H2 of COE), 25.6 (β–CH_2 of COE), 24.9 (ɣ–CH_2 of COE). ^{19}F NMR (282 MHz, C_6D_6) δ -74.7 (s, CF_3). We were unable to obtain satisfactory combustion analysis. NMR spectra are shown below.

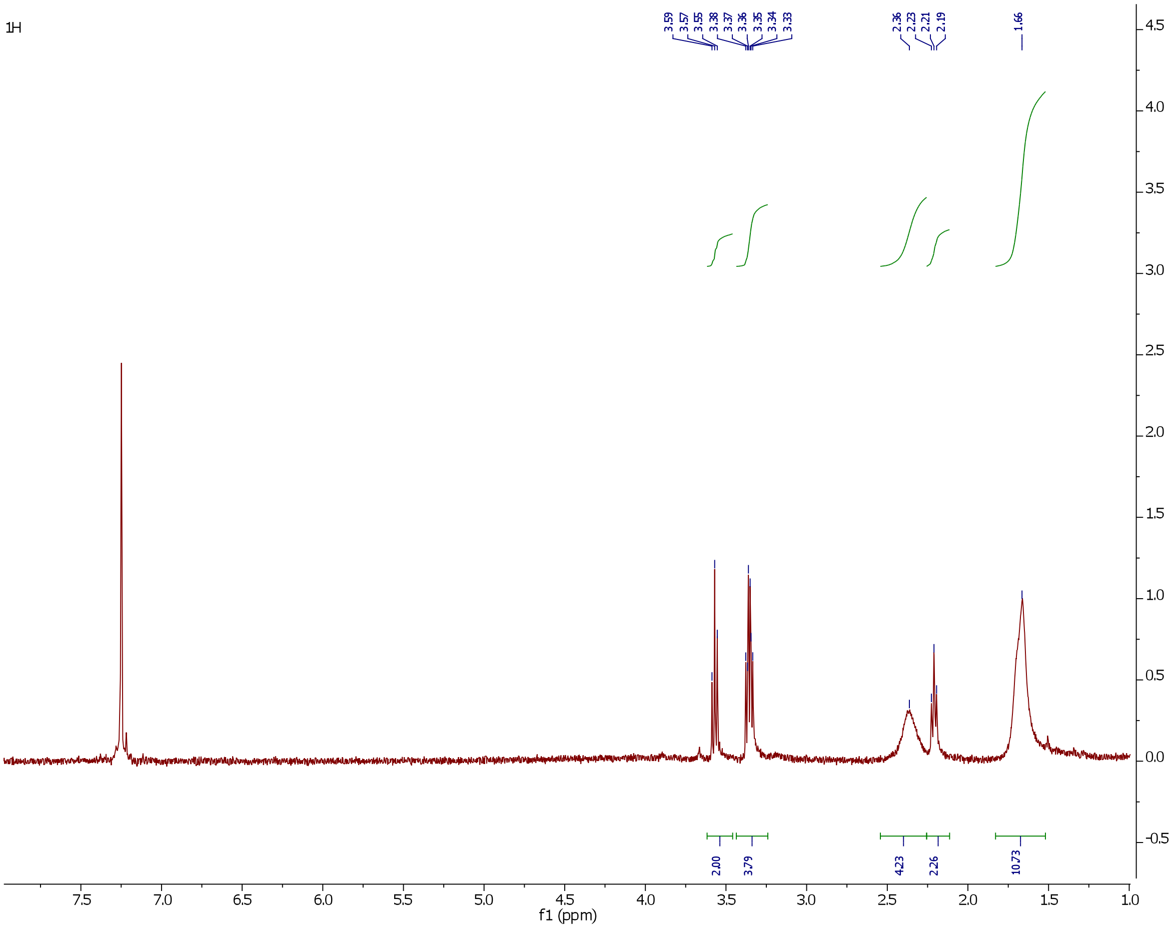

Figure S4. ^{1}H NMR spectrum of (BOZO)Rh(COE)(TFA) (**2**) in C_6D_6.

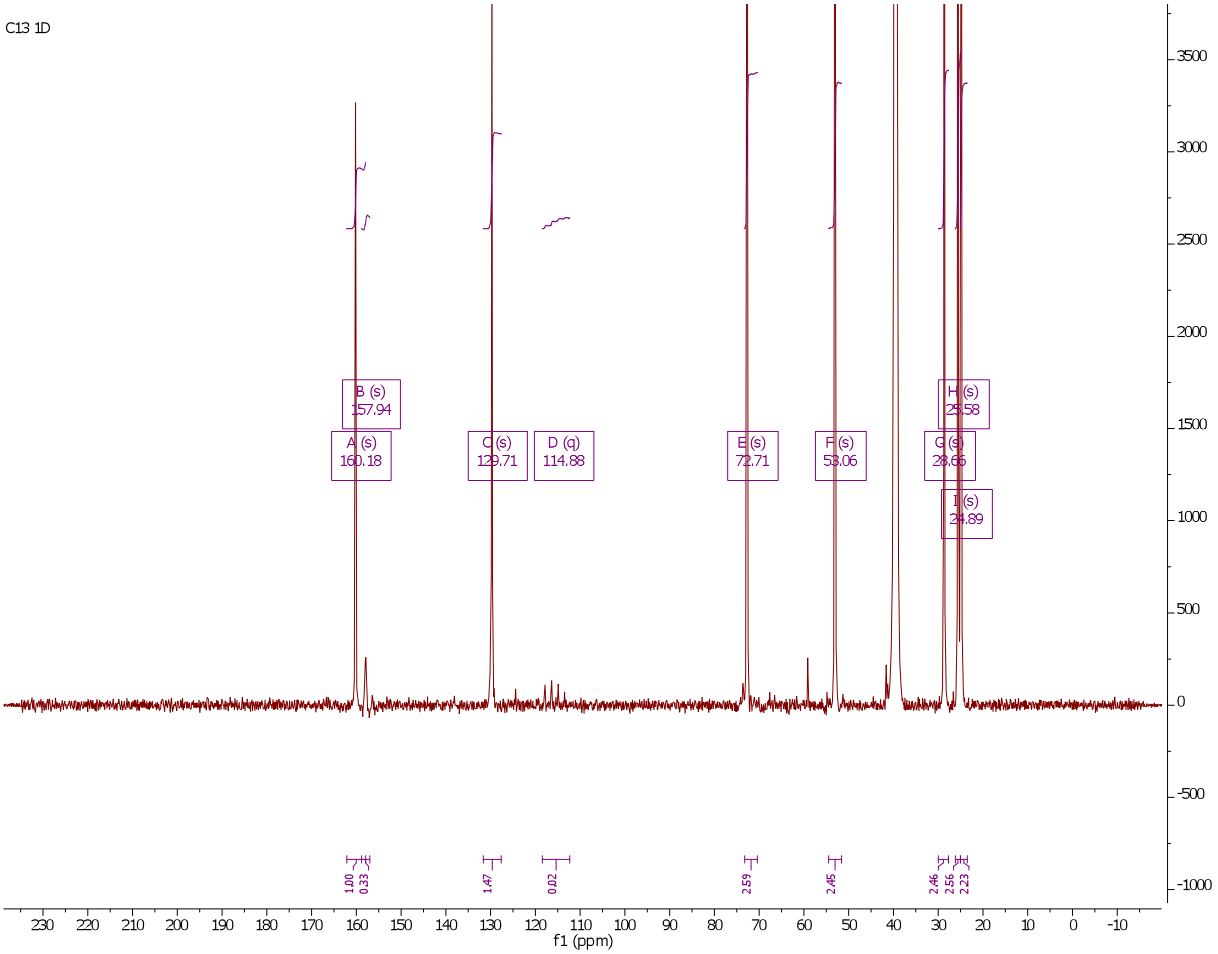

Figure S5. ^{13}C NMR spectrum of (BOZO)Rh(COE)(TFA) (**2**) in THF-d_8.

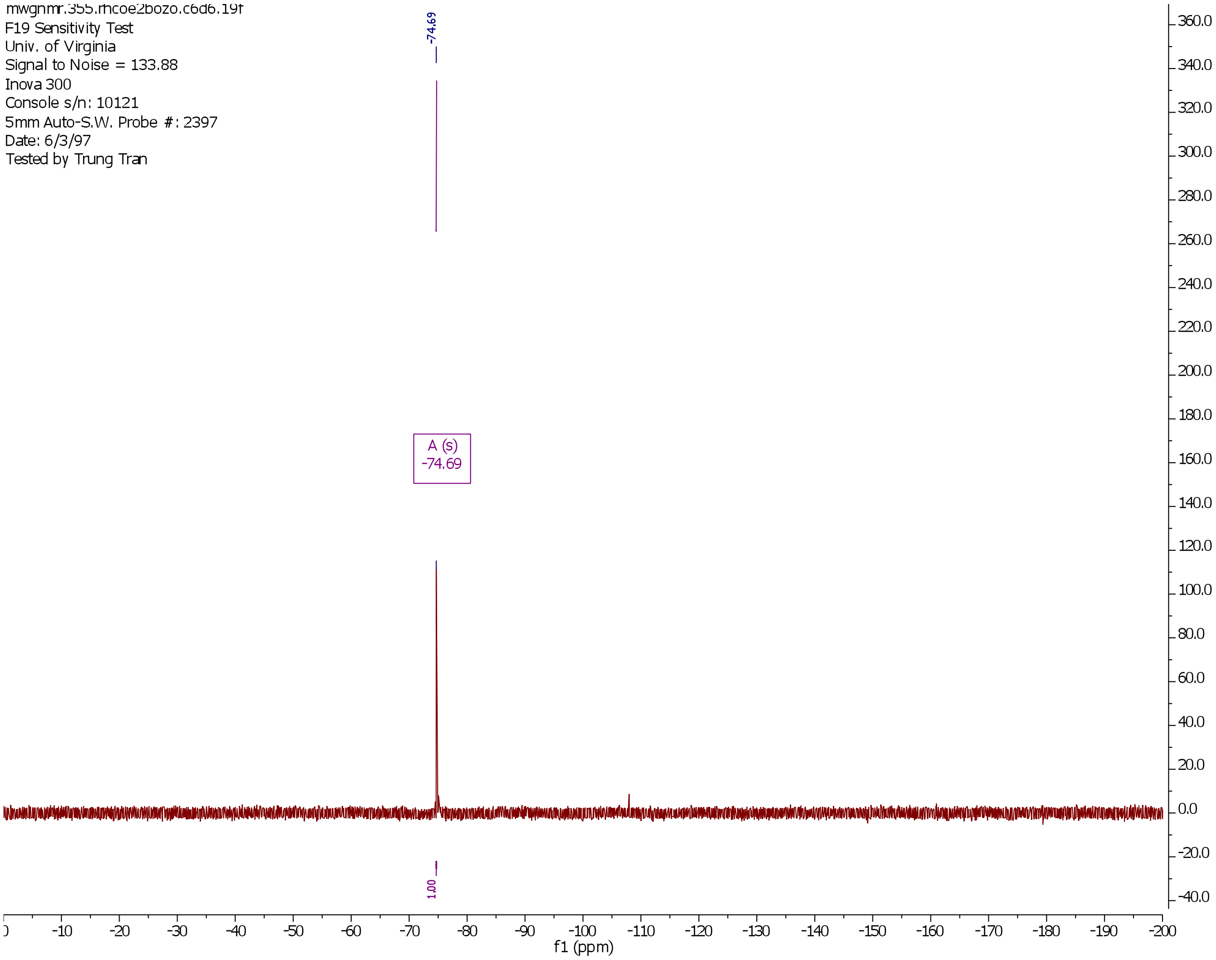

Figure S6. ^{19}F NMR spectrum of (BOZO)Rh(COE)(TFA) in C_6D_6.

Representative procedure for benzene H/D exchange. Stainless steel pressure reactors were used for H/D exchange reactions (see photographs below). All pressure reactors bottoms and stir bars were treated with 35% hydrogen peroxide, washed with acetone and dried before use. To a 2 mL pressure reactor was added a small stir bar. A stock solution was made by placing 7.7 mg (0.01 mmol of **1**) into a glass vial and dissolved in 6.58 mL (86 mmol) of [D_1] trifuoroacetic acid. Benzene (200 uL, 2.2 mmol) was then added to the stock solution. 1 mL of stock solution was added to each pressure reactor, which was sealed under N_2, pressurized with 800 psi argon, and placed in a heating block set to 150 °C. At the end of the reaction, the pressure reactor was cooled to room temperature, slowly vented, and opened. 1 uL of the reaction mixture was then analyzed by GC–MS.

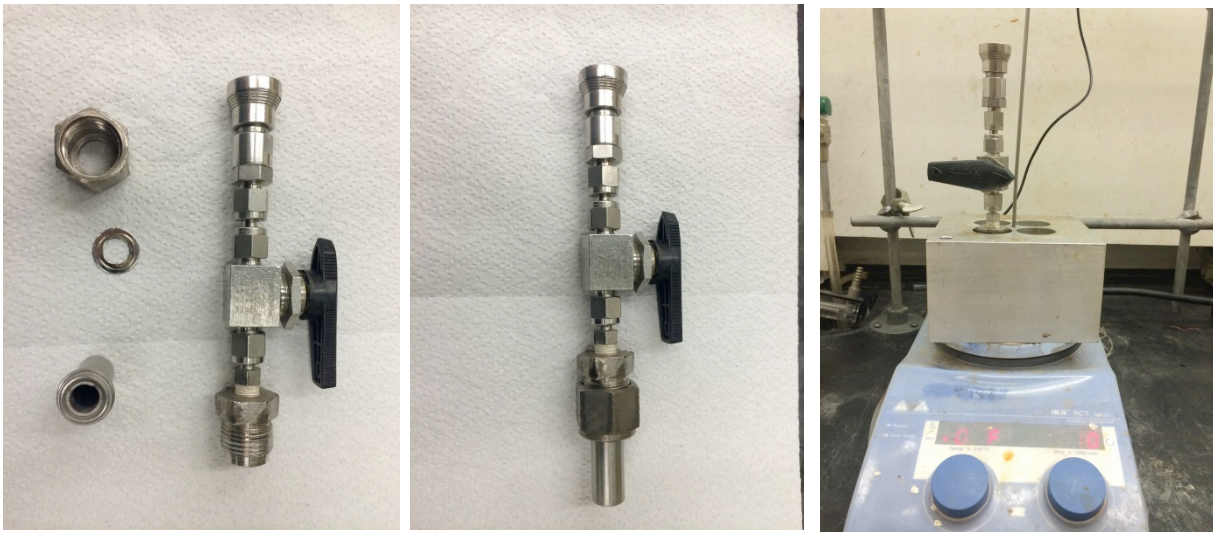

Figure S7. Pressure reactors used in H/D exchange. Left – Unassembled reactor parts. Middle - Assembled reactor. Right – Fully assembled reactor in aluminum heating block.

Representative procedure for toluene H/D exchange. To a glass vial, 7.7 mg (0.01 mmol) of (^{Fl}DAB)Rh(TFA)(coe) (**1**) was dissolved in 6.58 mL of trifluoroacetic acid and 200 uL of $[D_8]$ toluene. 0.5 mL of stock solution was put into a J-young NMR tube which had a capillary filled with $[D_6]$ -DMSO, and then sealed. The J-Young tube was put in an oil bath at 150 °C and monitored after 10 minutes.

Representative catalyst recycle experiments. A catalyst stock solution was made as follows: 7.7 mg of complex **1** are weighed into a glass screw cap vial, and then 6 mL of trifluoroacetic acid and 0.2 mL of C_6D_6 were added. A stir bar and 2 mL of stock solution were then put into glass pressure tubes and sealed with an O-ring and Teflon screw cap. These were placed in a preheated oil bath at 150 °C. After the set reaction time, the pressure tubes were cooled to room temperature and brought into the glove box. The reaction was analyzed using 1 uL of solution. The remainder of the solution was evaporated and the residue dried in vacuo and fresh trifluoroacetic acid and C_6D_6 were added. This process was repeated.

Computational methods

All quantum mechanical calculations were carried out using the Jaguar software version 7.6 developed by Schrödinger Inc. [4] Geometry optimizations were carried out on initial guess structures, and vibrational frequencies were gathered to confirm the optimized geometries as intermediates or transition states and to construct a free energy profile. Solvation energies were calculated using the PBF Poisson-Boltzmann implicit continuum solvation model [5] in Jaguar, with a dielectric constant of 8.55 and a probe radius of 2.451 Å for TFAH.

Geometry optimization and vibrational data were calculated using the B3LYP density functional [6] with a smaller basis set, whereas single point gas-phase and solvated energies were calculated using the M06 functional [7] and a larger basis set. Here the "smaller basis set" consists of a modified double-ζ Los Alamos basis set and pseudopotential [8] that includes *f* functions for rhodium [9], and the 6-31G** basis set [10] for the other atoms; whereas the "larger basis set" consists of the triple-ζ Los Alamos basis set and pseudopotential (LACV3P**++) modified to include *f* functions and diffuse functions for rhodium, and the 6-311G**++ basis set [11] for the other atoms.

The free energy for each molecular species in solution was calculated using the formula

$$G = Egas + \Delta Gsolv + ZPE + Hvib + 6kT - TSvib + 0.54Strans + Srot - 14.3 \text{ e.u.} + 7.98 \text{ e.u.}$$

where the last term is an empirical approximation of the change in the translational and rotational entropy of the molecule between the gas phase and the solution phase (due to the finite librational frequencies) derived from Wertz [12].

For pure liquids (e.g., trifluoroacetic acid), the Gibbs free energy was calculated using the formula

$$Gliquid = Egas + ZPE + Htot - TStot + \Delta Ggas \rightarrow liquid$$

where $\Delta Ggas\rightarrow liquid=Gliquid-Ggas(1\text{ atm})$ is the free energy of condensation to liquid from 1 atm gas. We can solve for this by noting that

$\Delta Ggas\rightarrow liquid=\Delta Gexp+\Delta Ggas\rightarrow solv,$

where $\Delta Gexp=GgasP-Ggas(1\text{ atm})$ is the expansion of the gas from 1 atm to the vapor pressure P, and $\Delta Ggas\rightarrow solv$ is the condensation of gas to liquid. Since a liquid is by definition at equilibrium with its vapor pressure, $\Delta Ggas\rightarrow solv=0$, and we thus have

$\Delta Ggas\rightarrow liquid=GgasP-Ggas1\text{ atm}=RTlnP1\text{ atm}.$

We can find the vapor pressure P at a given temperature using the Antoine Equation:

$log10P=A-BC+T,$

where the empirical parameters A, B, and C vary with the solvent and temperature range and were taken from table S1. Calculations were performed at nine temperature levels spaced by 25 K from 298.15 K to 498.15 K.

Table S1. Antoine equation parameters used for trifluoroacetic acid and water at each temperature point investigated. Numbers taken from [13] and are set such that *P* will be measured in bar.

Temperature	Trifluoroacetic acid		
	A	B	C
298.15 K	3.33963	1267.252	-52.958
323.15 K	3.33963	1267.252	-52.958
348.15 K	3.33963	1267.252	-52.958
373.15 K	3.33963	1267.252	-52.958
398.15 K	3.33963	1267.252	-52.958
423.15 K	3.33963	1267.252	-52.958
448.15 K	3.33963	1267.252	-52.958
473.15 K	3.33963	1267.252	-52.958
498.15 K	3.33963	1267.252	-52.958

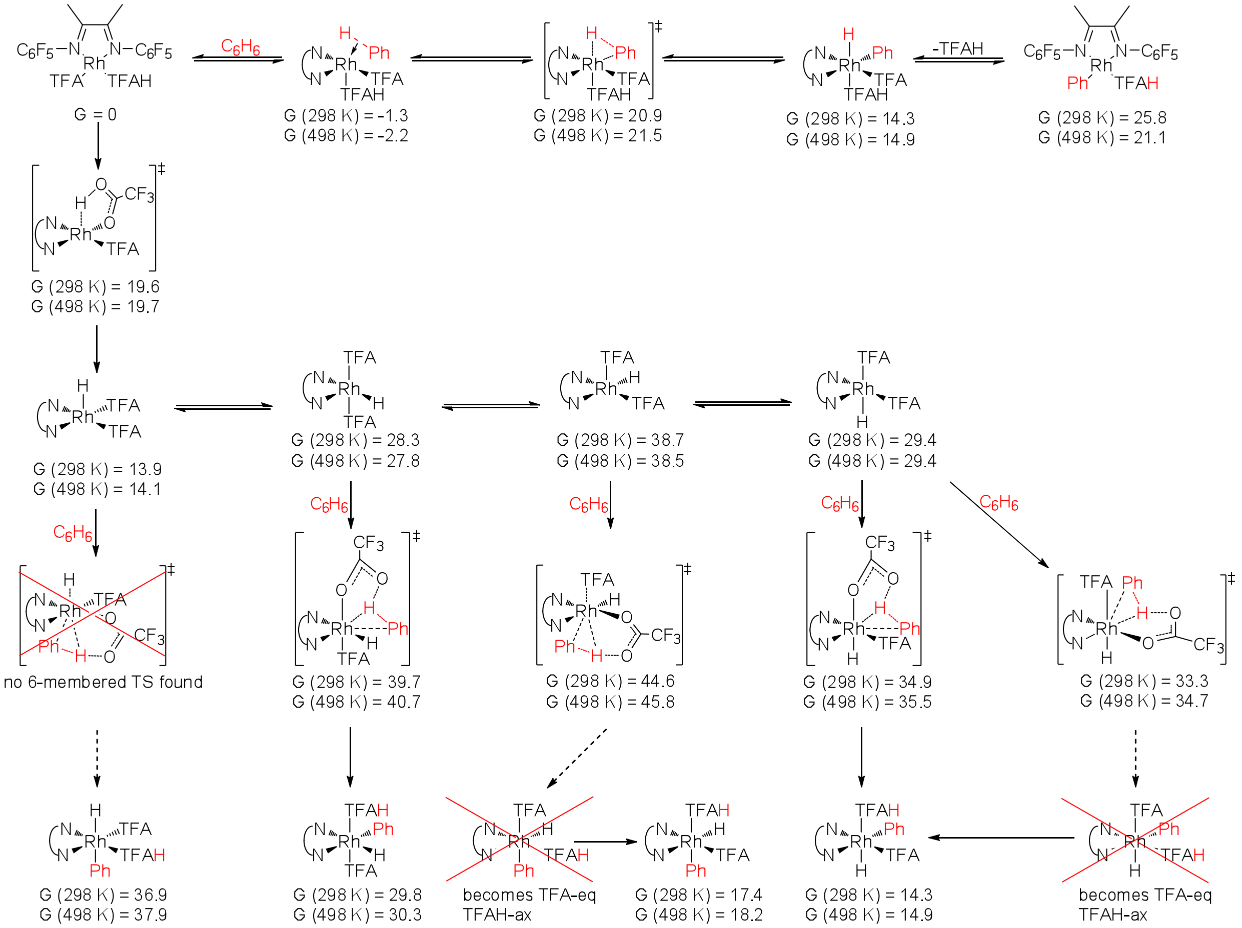

Scheme S1. The (^{F1}DAB)Rh(TFA)(TFAH) (**3**) activates benzene with 22.2-23.7 kcal/mol barrier (298-498 K). Top row: direct oxidative addition of benzene by Rh^{I}. Elsewhere: internal oxidative addition of **3** followed by benzene coordination. All free energies in kcal/mol.

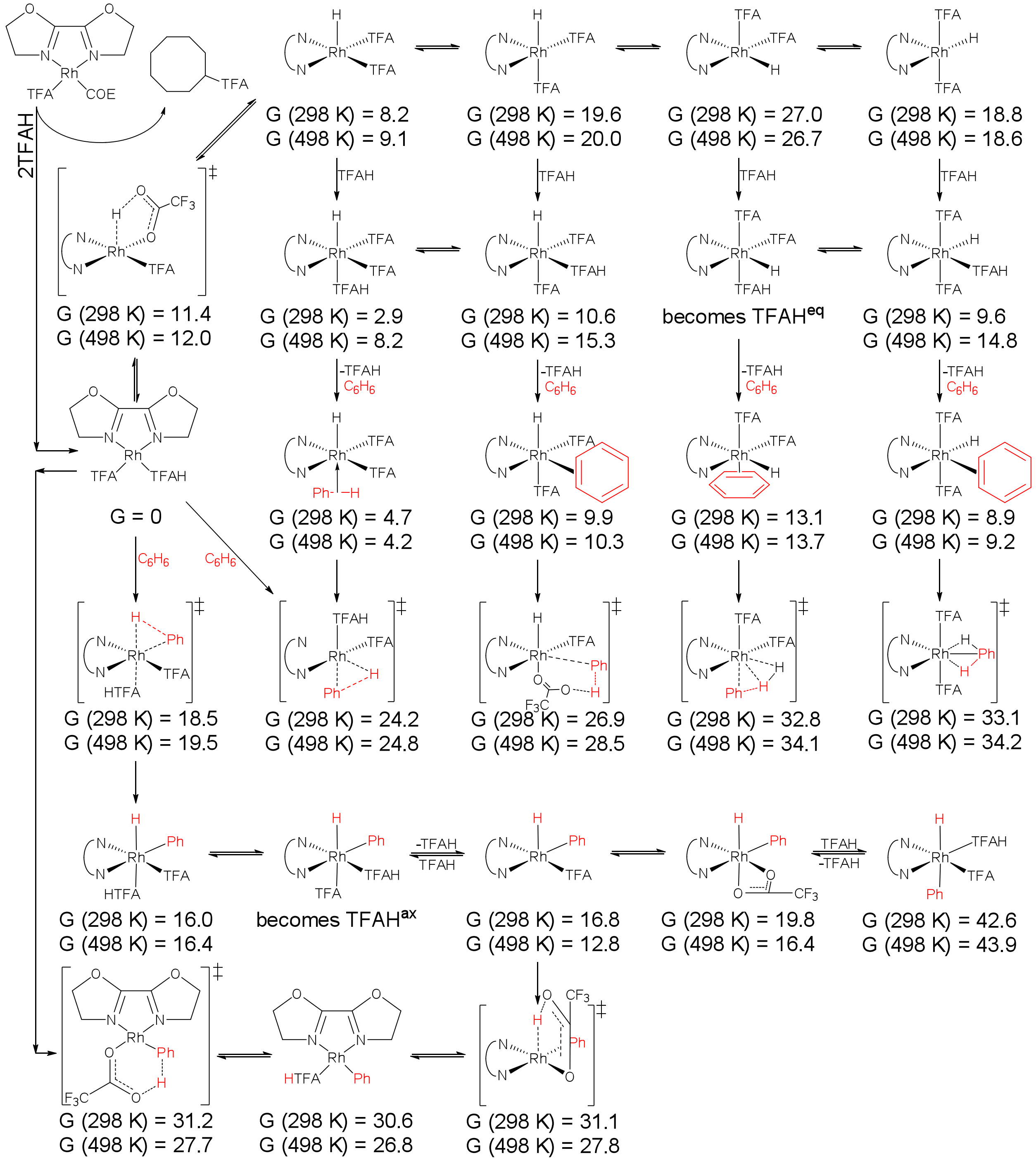

Scheme S2. The (BOZO)Rh(TFA)(TFAH) complex 4 activates benzene with 18.5-19.5 kcal/mol barrier (298-498 K). First column, 2nd and 3rd TSs: Direct reaction of benzene by Rh^I, *via* oxidative addition or concerted intramolecular electrophilic substitution (IES). Elsewhere: internal oxidative addition followed by benzene coordination. All free energies in kcal/mol.

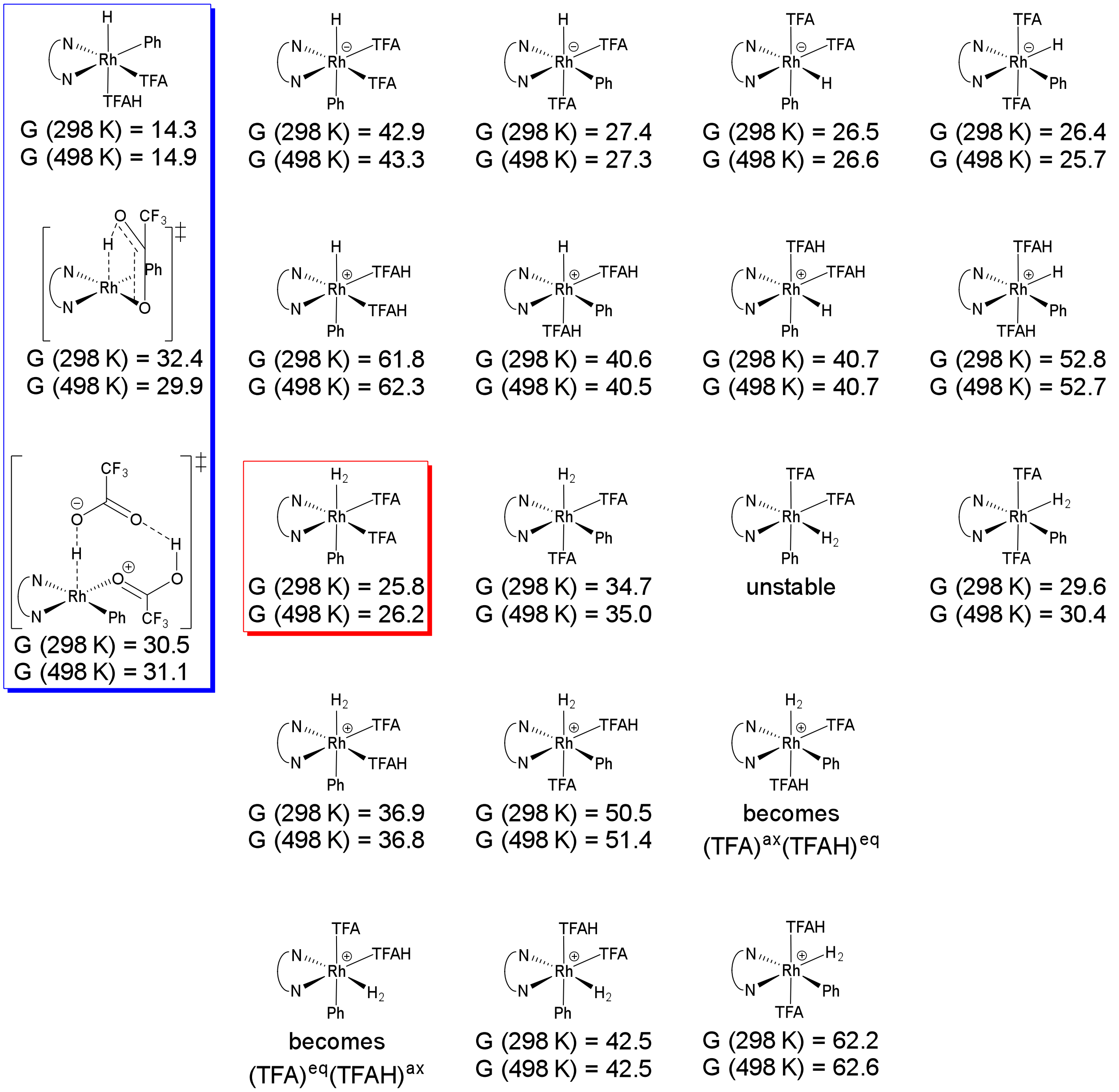

Figure S8. (^{F1}DAB)Rh complexes (from **3**) with H_2. The red box shows the lowest energy (^{F1}DAB)Rh(η^2-H_2) species found. The blue box shows the lowest isomeric (^{F1}DAB)Rh(H)(Ph)(TFA)(TFAH) species for comparison, as well two internal protonation transition states. Although the red box species is lower in energy than the internal protonation transition states, it can only be accessible through higher energy species. Hence the pathway *via* H_2 adducts is not viable.

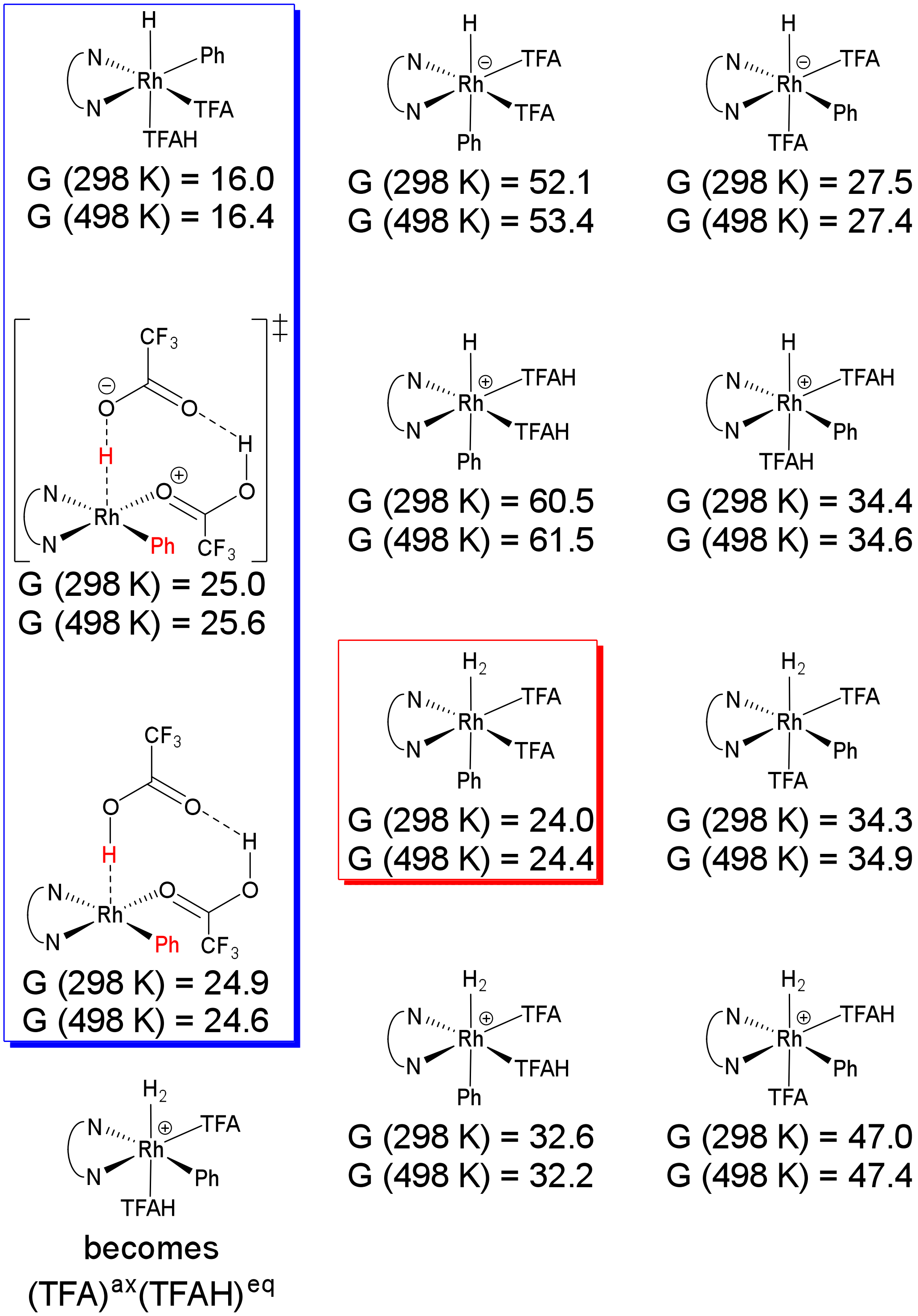

Figure S9. (BOZO)Rh complexes (from **4**) with H_2. The red box shows the lowest energy (BOZO)Rh(η^2-H_2) species found. The blue box shows the lowest isomeric (BOZO)Rh(H)(Ph)(TFA)(TFAH) species for comparison, as well two internal protonation transition states. Although the red box species is lower in energy than the internal protonation transition states, it can only be accessible through higher energy species. Hence the pathway *via* H_2 adducts is not viable.

References

1. Khusniyarov, M. M.; Harms, K.; Burghaus, O.; Sundermeye, J.; *Eur. J. Inorg. Chem.* **2006**, 2985–2996 .
2. Schrock, R.R.; Osborn, J. A.; *J. Am. Chem. Soc.* **1971,** 93, 3089.
3. Young, K. J. H.; Meier, S. K.; Gonzales J. M.; Oxgaard, J.; Goddard, W. A. III.; Periana, R. A.; *Organometallics* **2006,** *25,* 4734-4737 .
4. *Jaguar, version 7.6*; Schrödinger, LLC: New York, NY, 2007.
5. a) Tannor, D. J.; Marten, B.; Murphy, R.; Friesner, R. A.; Sitkoff, D.; Nicholls, A.; Ringnalda, M.; Goddard, W. A.; Honig, B. *J. Am. Chem. Soc.* **1994**, *116*, 11875-11882; b) Marten, B.; Kim, K.; Cortis, C.; Friesner, R. A.; Murphy, R. B.; Ringnalda, M. N.; Sitkoff, D.; Honig, B. *J. Phys. Chem*. **1996**, *100*, 11775-11788.
6. a) Becke, A. D. *Phys. Rev. A* **1998**, *38*, 3098-3100; b) Becke, A. D. *J. Chem. Phys.* **1993**, *98*, 5648-5652; c) Lee, C. T.; Yang, W. T.; Parr, R. G. *Phys. Rev. B* **1988**, *37*, 785-789.
7. a) Zhao, Y.; Truhlar, D. G. *Theor. Chem. Acc.* **2008**, *120*, 215-241; b) Zhao, Y.; Truhlar, D. G. *Acc. Chem. Res.* **2008**, *41*, 157-167.
8. Hay, P. J.; Wadt, W. R. *J. Chem. Phys*. **1985**, *82*, 299-310.
9. Martin, J. M. L.; Sundermann, A. *J. Chem. Phys.* **2001**, *114*, 3408-3420.
10. a) Hehre, W. J.; Ditchfield, R; Pople, J. A. *J. Chem. Phys.* **1972**, *56*, 2257-2261; b) Francl, M. M.; Pietro, W. J.; Hehre, W. J.; Binkley, J. S.; Gordon, M. S.; Defrees, D. J.; Pople, J. A. *J. Chem. Phys.* **1982**, *77*, 3654-3665.
11. a) Clark, T.; Chandrasekhar, J.; Spitznagel, G. W.; Schleyer, P. V. *J. Comput. Chem.* **1983**, *4*, 294; b) Krishnan, R.; Binkley, J. S.; Seeger, R.; Pople, J. A. *J. Chem. Phys.* **1980**, *72*, 650-654.
12. Wertz, D. H. *J. Am. Chem. Soc.* **1980**, *102*, 5316-5322.
13. Kreglewski, A. *Bull. Acad. Pol. Sci. Ser. Sci. Chim.* **1962**, *10*, 11-12, 629-633.